

# Supporting Information File

## Azacrown Ether-Copper(II)-Hexanoate Complexes. From Monomer to 1-D Metal Organic Polymer

Kamil Wojciechowski<sup>\*1,2</sup>, Anna Bitner<sup>1</sup>, Gérald Bernardinelli<sup>3</sup>, Marcin Brynda<sup>4</sup>

1) Department of Analytical Chemistry, Warsaw University of Technology, Noakowskiego 3,  
00-664 Warsaw, Poland

2) Analytical and Biophysical Environmental Chemistry (CABE) Department of Analytical,  
Inorganic and Applied Chemistry, Sciences II, 30 quai E. Ansermet, CH-1211 Geneve 4, Suisse

3) Laboratory of X-ray Crystallography, University of Geneva. 24, quai E. Ansermet, CH-1211  
Geneva 4, Switzerland

4) Department of Chemistry, University of California, Davis. One Shields Avenue, 95616 Davis,  
USA

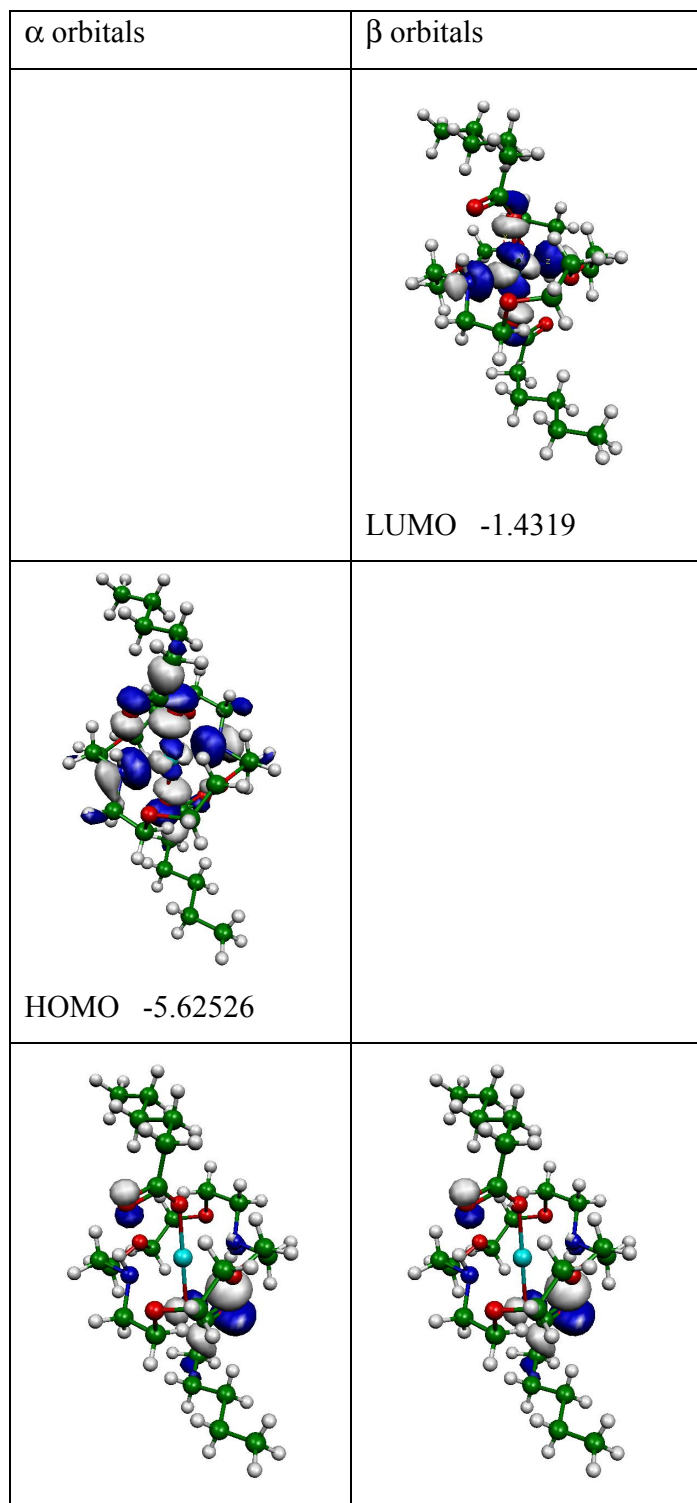
S1.

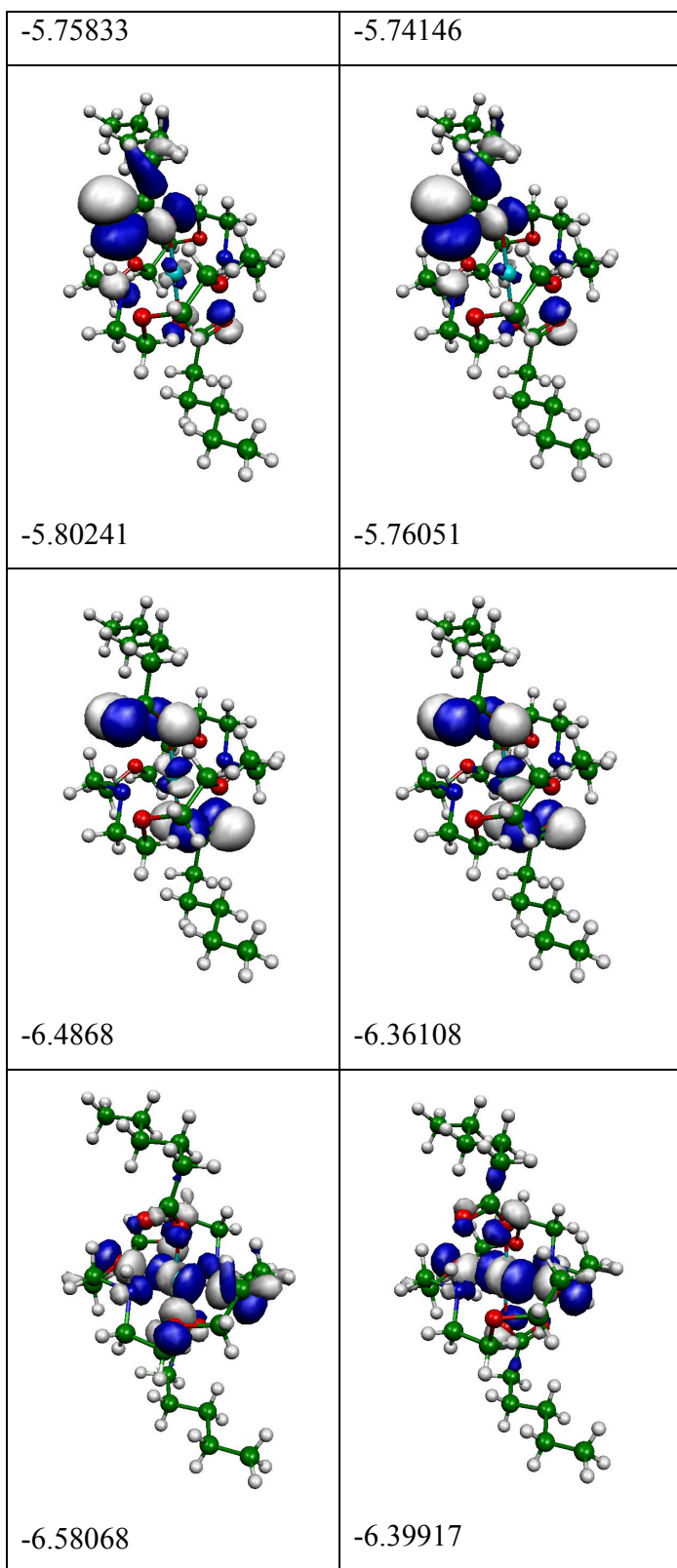
Bond Distances [Å]			
Cu-O2	2.620(2)	Cu-N1	2.037(3)
Cu-O1a	1.975(3)	O1-C2	1.437(5)
O1-C3	1.437(4)	O2-C4	1.439(4)
O2-C5	1.424(5)	N1-C1	1.459(5)
N1-H01	.85(4)	N1-C6'	1.484(4)
C1-C2	1.500(5)	C3-C4	1.491(6)
C5-C6	1.515(5)	O1a-C1a	1.279(4)
O2a-C1a	1.250(5)	C1a-C2a	1.438(8)
C2a-C3a	1.480(9)	C3a-C4a	1.523(9)
C4a-C5a	1.521(9)	C5a-C6a	1.50(1)
Bond Angles [°]			
O2-Cu-N1	101.46(9)	O2-Cu-O1a	84.37(9)
O2-Cu-O2'	180.0000	O2-Cu-N1'	78.54(9)
O2-Cu-O1a'	95.63(9)	N1-Cu-O1a	92.2(1)
N1-Cu-O2'	78.54(9)	N1-Cu-N1'	180.0(2)
N1-Cu-O1a'	87.8(1)	O1a-Cu-O2'	95.63(9)
O1a-Cu-N1'	87.8(1)	O1a-Cu-O1a'	180.0(6)
O2'-Cu-N1'	101.46(9)	O2'-Cu-O1a'	84.37(9)
N1'-Cu-O1a'	92.2(1)	C2-O1-C3	113.9(3)
Cu-O2-C4	122.1(2)	Cu-O2-C5	95.2(2)
C4-O2-C5	112.2(3)	Cu-N1-C1	118.2(2)
Cu-N1-H01	91(2)	Cu-N1-C6'	110.1(2)
C1-N1-H01	115(3)	C1-N1-C6'	112.2(3)
H01-N1-C6'	108(2)	N1-C1-C2	111.9(3)
O1-C2-C1	107.9(3)	O1-C3-C4	113.0(3)
O2-C4-C3	110.4(3)	O2-C5-C6	107.5(3)
C5-C6-N1'	112.8(3)	Cu-O1a-C1a	134.9(3)

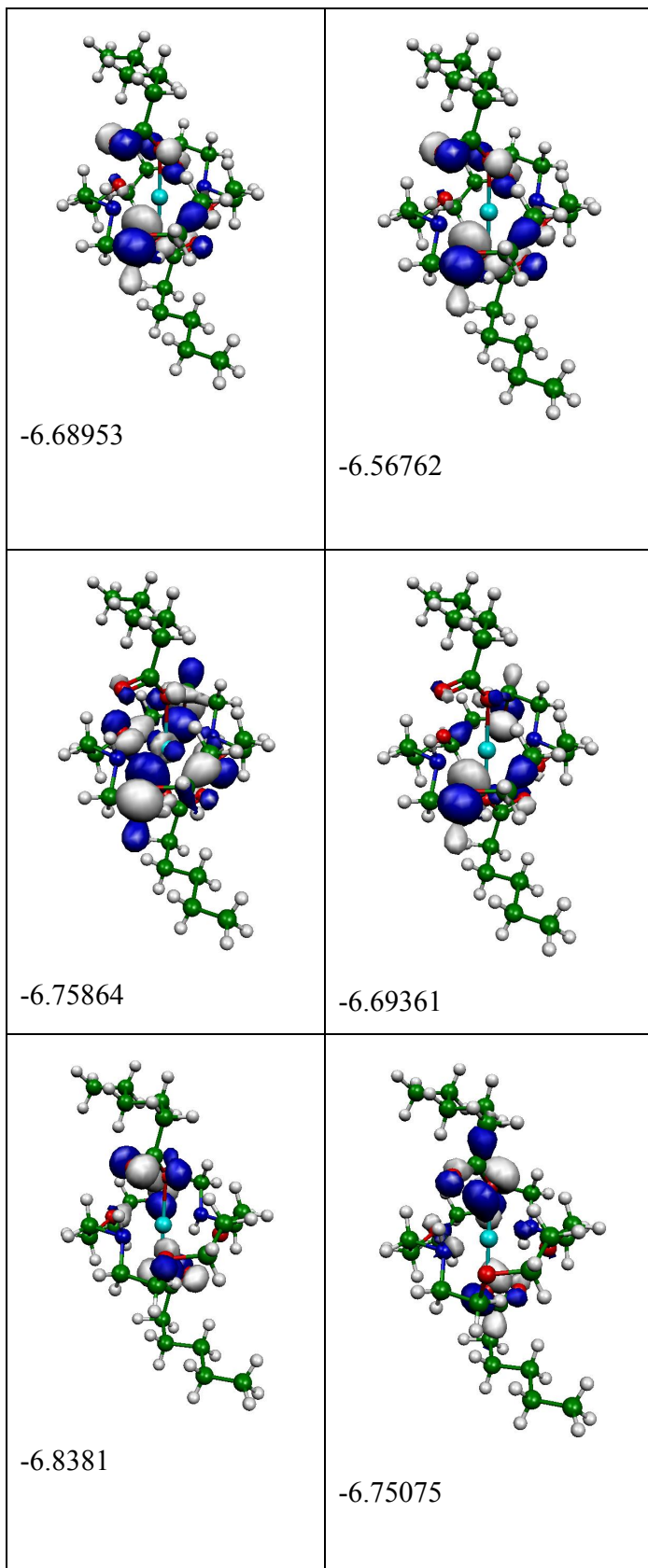
O1a-C1a-O2a	124.9(4)	O1a-C1a-C2a	117.8(4)
O2a-C1a-C2a	117.2(4)	C1a-C2a-C3a	114.4(5)
C2a-C3a-C4a	116.5(5)	C3a-C4a-C5a	113.5(5)
C4a-C5a-C6a	115.4(7)	Cu-H01-N1	66(2)
Dihedral Angles [°]			
C3-O1-C2-C1	153.3(3)	C2-O1-C3-C4	-92.1(4)
C5-O2-C4-C3	165.9(3)	C4-O2-C5-C6	176.8(3)
H01-N1-C1-C2	54(3)	C6-N1-C1-C2'	178.7(3)
N1-C1-C2-O1	-58.2(4)	O1-C3-C4-O2	67.2(4)
O2-C5-C6-N1'	-71.6(4)	O1a-C1a-C2a-C3a	-44.7(7)
O2a-C1a-C2a-C3a	133.4(5)	C1a-C2a-C3a-C4a	-59.5(8)
C2a-C3a-C4a-C5a	-179.3(6)	C3a-C4a-C5a-C6a	178.3(7)
Hydrogen bonds			
N1-H01 = 0.85(4) Å		H01...O2a = 1.98(4) Å	
N1...O2a = 2.787(5) Å		N1-H01...O2a = 157(4) °	
(') = -x , 1-y , 1-z			
Cu is in a special position 2a in the centre of inversion at (0 , ½ , ½ )			

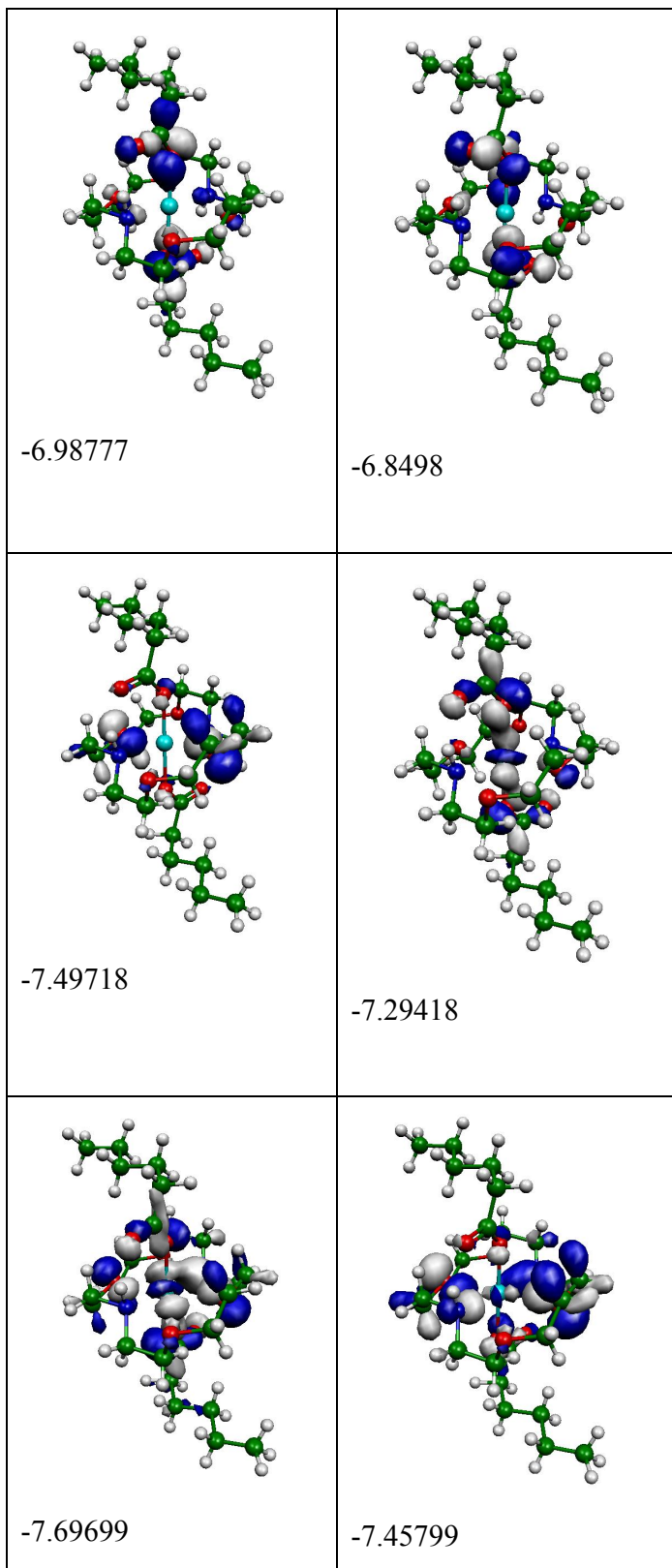
Table S1. Selected geometrical parameters for complex **1**.

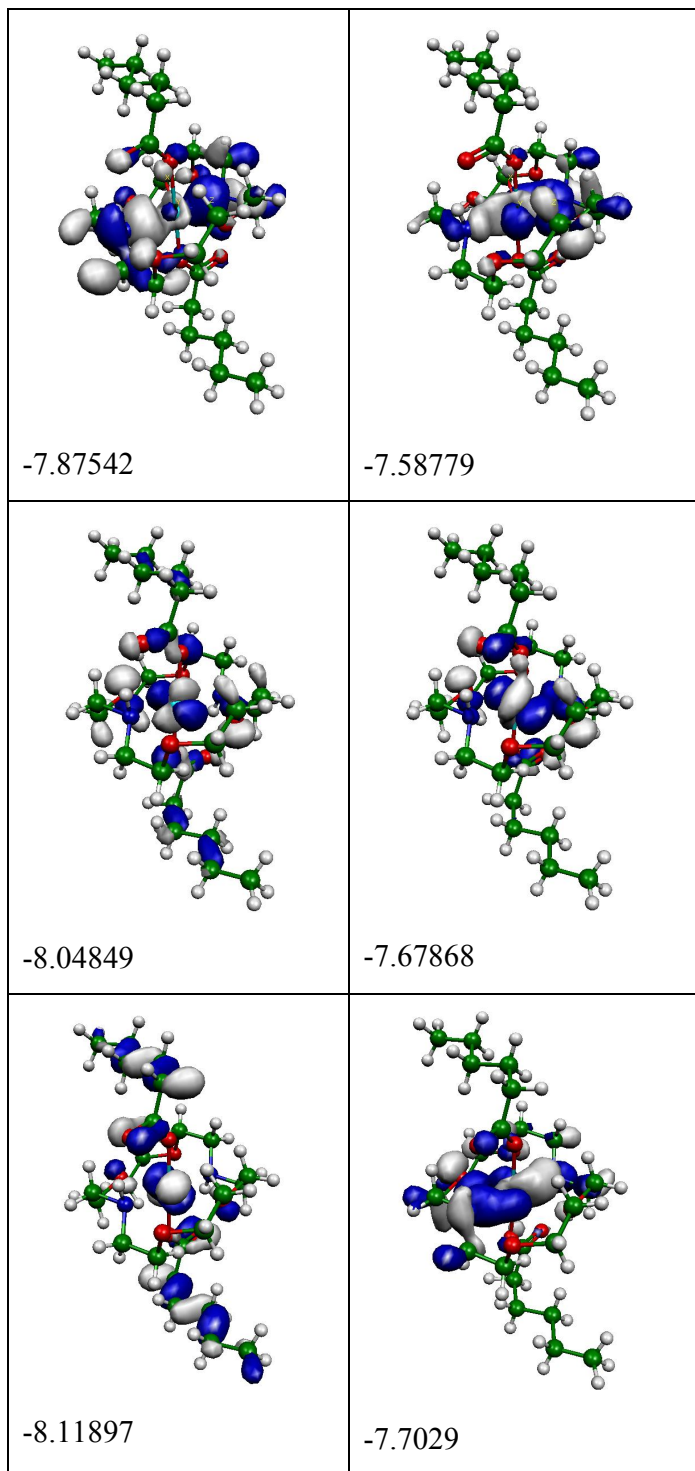
S2.

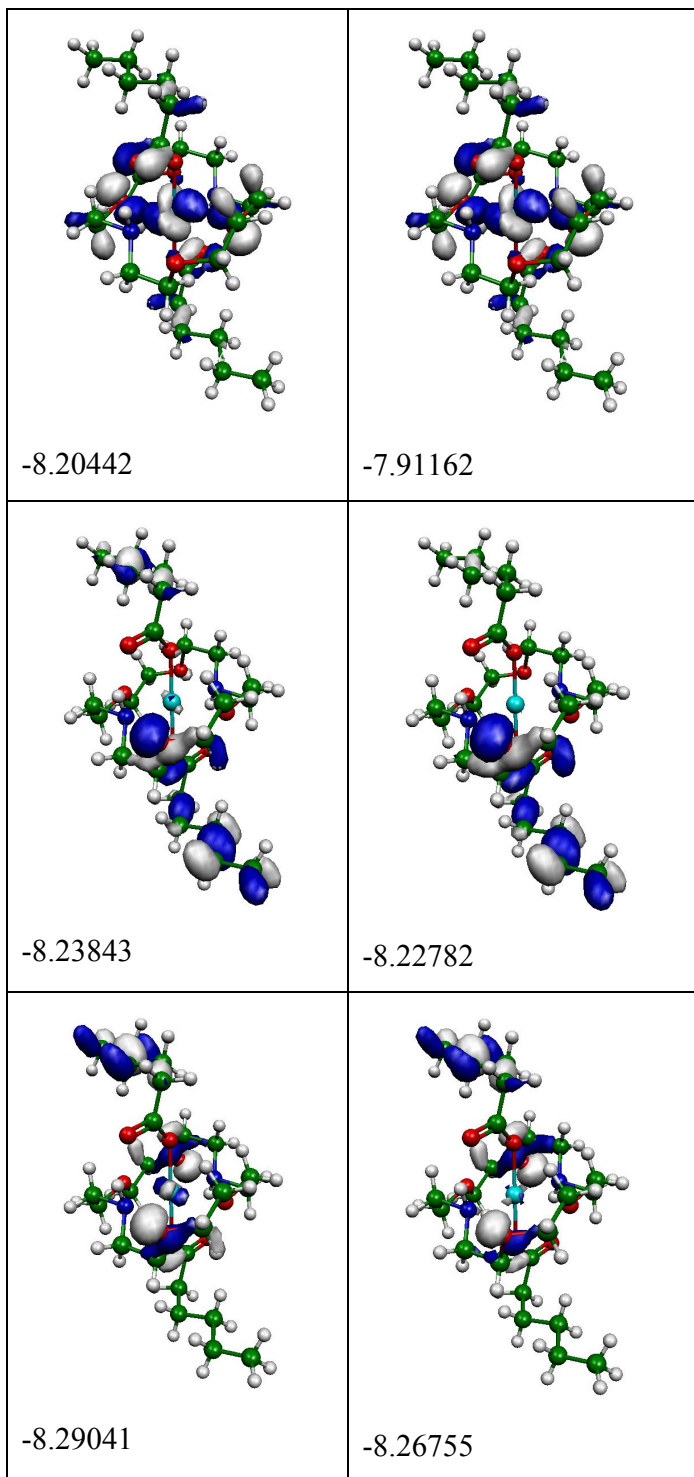












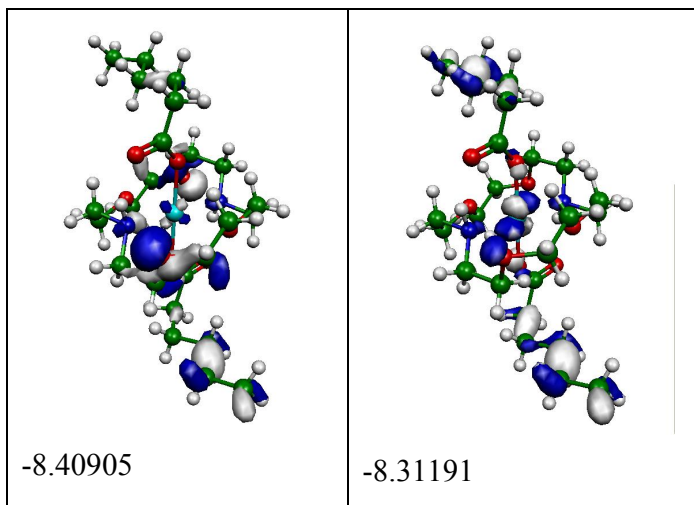


Table S2. Contour plots of the  $\alpha$  and  $\beta$  frontier Kohn-Sham orbitals for complex 1, with the corresponding energies in [eV].

S3.

Bond	Bond order
Cu-O1a	0.548
Cu-O1b	0.544
Cu-O1	0.161
Cu-O2	<0.1
Cu-N1	0.395
Cu-N2	0.418

Table. S3. Calculated Mayer bond orders for selected atoms neighbouring copper in 1 (see Fig. 4 for the numbering scheme).

#### Contribution of axial oxygens to the molecular *g*-matrix.

To facilitate the understanding of the electronic structure of complex 1 the calculations were also performed on its simplified model S1, in which the hexanoate groups were replaced by acetates and the nitrogens and oxygen atoms of the azacrown ether by ammonia and water molecules, respectively. The electronic structure of such

simple model is essentially the same as that of **1**. Fig. S4a shows the unpaired electron density with clear maxima regions corresponding to a  $d(x^2-y^2)$  orbital on copper and on surrounding nitrogen and two acetate oxygens, as compared to almost identical spin density computed for **1** (Fig S4b).

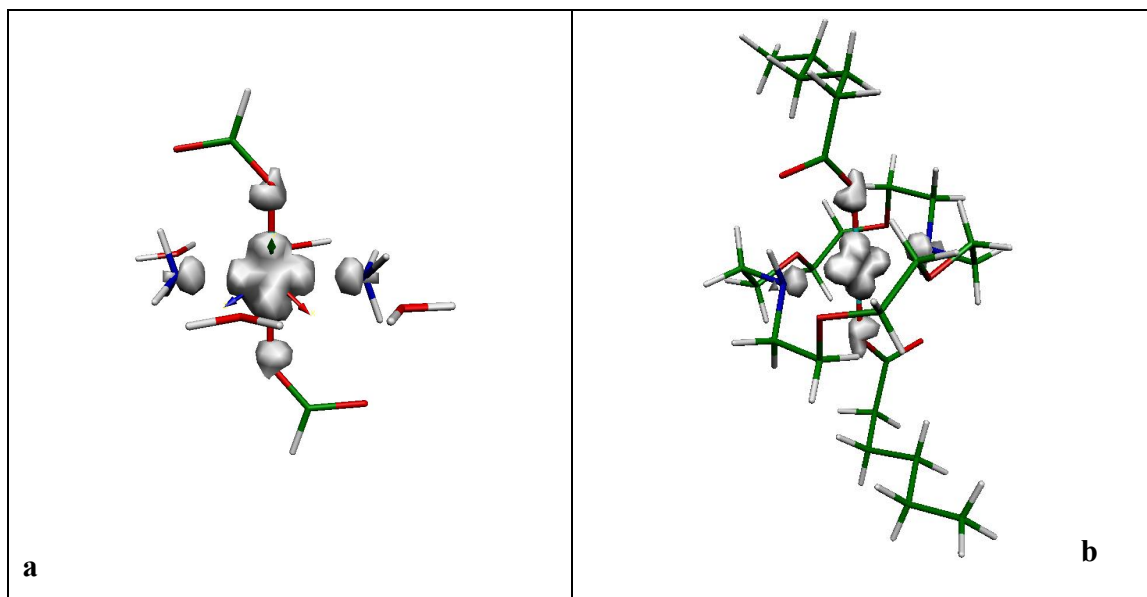


Fig. S4. (a) The unpaired electron density of a simplified complex **S1** (with the hexanoate groups replaced by acetates and the nitrogen and oxygen atoms of the azacrown ether by ammonia and water molecules, respectively). (b) The unpaired electron density of a complete complex **1**.

The symmetry-dictated overlap of the major MO's components for the other  $d$  copper orbitals are schematised below. Since the geometry of **1** differs from the perfectly square planar  $D_{4h}$ , this lower symmetry results in only limited orbital overlap between the copper  $d$  orbitals and the  $p_{x,y,z}$  orbitals of oxygen and nitrogen. The most important AOs types of the ACE and carboxylate fragments participating in the MOs of the complex **1** molecule are schematically depicted in Table S5. With the ACE molecule lying in the  $zy$  plane, it is clear from Fig S4 that the  $p_n$  orbitals of nitrogen atoms of ACE interact mostly with the  $d(z^2)$ ,  $d(zy)$  and especially with  $d(x^2-y^2)$  of copper, while the ACE oxygen atoms show interactions with the  $d(z^2)$  and  $d(zy)$  orbitals only. In contrast, the carboxylic oxygen

$O^{COO}p_n$  orbitals interact principally with  $d(xy)$ ,  $d(xz)$  and  $d(x^2-y^2)$  orbitals of the metal centre. From the EPR point of view the implication of such interaction is that the Jahn-Teller distortion along the z axis would modulate the SOMO character of the complex and consequently its  $g$  values.

Fragment			
$O^{COO}p_x$		$O^{\text{ether}}p_z$	
$O^{COO}p_y$		$N^{\text{ether}}p_x$	
$O^{COO}p_z$		$N^{\text{ether}}p_y$	

Table S5. Main AOs types of the ACE and carboxylate fragments participating in the MOs of complex **1**.

The fact that the reduced model **M1** reproduces well the most important features of **1**, prompted us to perform calculations on this model to monitor the changes in the  $g$ -matrix upon elongation of the  $O_{\text{ACE}}\text{-Cu}\text{-}O_{\text{ACE}}$  fragment. The results of these calculations are presented in Figure S6. In addition, we have also computed the atomic contribution of the  $O_{\text{ACE}}$  to the Paramagnetic Spin Orbit (PSO) term of the  $g$ -matrix (Fig S7) using extended output of the ORCA program as implemented for the  $g$ -matrix computation. For the experimental Cu-O distances ( $\sim 2.6$  Å) the differences in the  $g$ -matrix elements ( $\Delta g$ ) are

less than 0.010 for all three principal values. The paramagnetic spin-orbit contribution of the axial oxygens to the  $g$ -matrix is very small ( $10^{-6}$  to  $10^{-5}$ ), as compared to two other oxygen atoms and the nitrogens, which exhibit contributions of order of  $10^{-4}$  to  $10^{-3}$ .

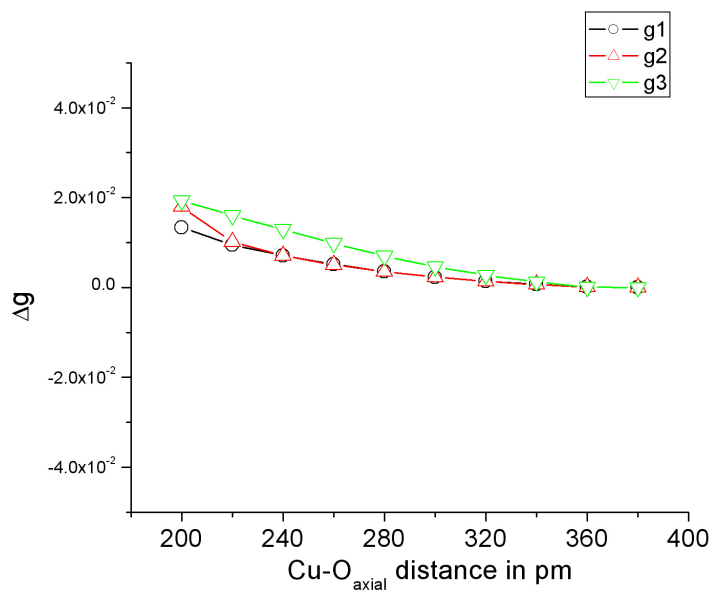


Fig. S6. Variation of the  $g$ -matrix principal components computed on simplified complex S1 for the range of the C-O<sub>ACE</sub> distances 2.0 to 3.6 Å.

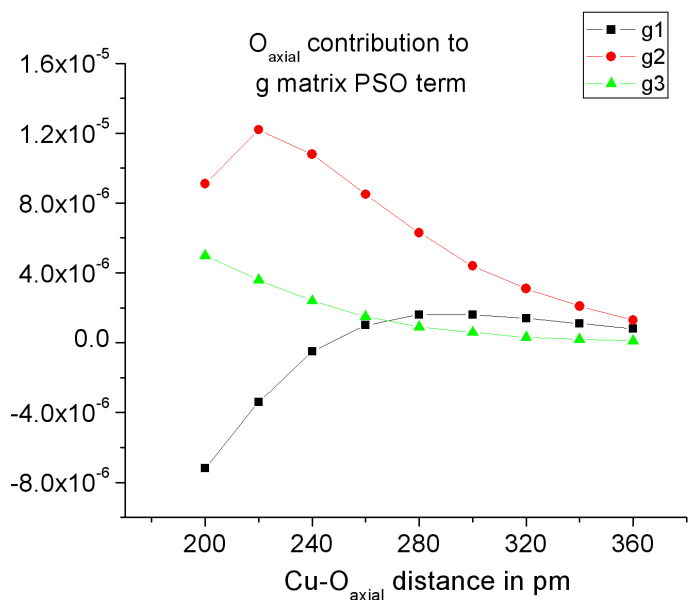


Fig. S7. Atomic contribution of the O<sub>axial</sub> into the g-matrix PSO term computed on simplified complex **S1** for the range of the C-O<sub>axial</sub> distances 2.0 to 3.6 Å.